JOC Article

Synthesis of Nonaphenylenes and Dodecaphenylenes Using Electron-Transfer Oxidation of Lipshutz Cuprates and Formation of Nanostructural Materials from Hexadodecyloxynonaphenylene

M. Jalilur Rahman, Jun Yamakawa, Aoi Matsumoto, Hideo Enozawa, Tohru Nishinaga, Kenji Kamada,† and Masahiko Iyoda*

Department of Chemistry, Graduate School of Science and Engineering, Tokyo Metropolitan University, Hachioji, Tokyo 192-0397, Japan, and Photonic Research Institute, National Institute of Advanced Industrial Science and Technology (AIST), AIST Kansai Center, Ikeda, Osaka 563-8577, Japan

iyoda@tmu.ac.jp

Received April 10, 2008

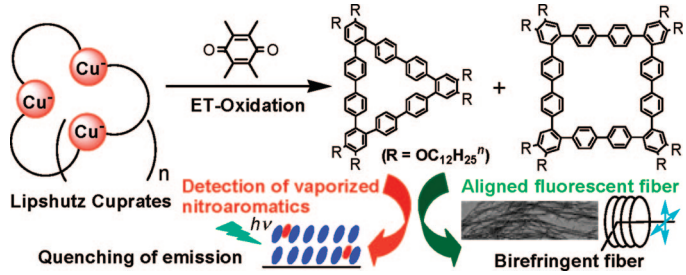

Nonaphenylenes and dodecaphenylenes have been synthesized by using electron-transfer oxidation of Lipshutz cuprates with duroquinone. Oxidation of the Lipshutz cuprate derived from 4,4″-dibromo-*o*-terphenyl **3a** in THF produced nonaphenylene **1a** in 46% yield, whereas the similar oxidation of the Lipshutz cuprates derived from 4,4″-diiodo-4′,5′-dialkyl-*o*-terphenyls **3b**−**d** in ether afforded the corresponding nonaphenylenes **1b**−**d** and dodecaphenylenes **2b**−**d** in moderate total yields. In the case of 4,4″-diiodo-4′,5′-didodecyloxy-*o*-terphenyl **3e** as the starting material, oxidation of the corresponding Lipshutz cuprate in ether or THF only led to the formation of nonaphenylene **1e**. Both nonaphenylenes **1a**−**e** and dodecaphenylenes **2b**−**d** are unreactive to light, atmospheric oxygen, and prolonged heating. These oligophenylenes showed strong UV absorption and fluorescent emission and exhibited some redox properties on CV analysis. Moreover, hexadodecyloxynonaphenylene **1e** exhibits different nanostructures on the surface and in solution to form a film by casting a solution of **1e** in cyclohexane, benzene, chloroform, THF, or diisopropyl ether (IPE) and nanofibers from IPE−MeOH (1:1), indicating different absorption and emission spectra and XRD patterns. The absorption maxima of THF solution, fiber, and film are in the order of **1e** film (315 nm) > fiber (302 nm) > solution (295 nm), whereas the emission maxima are in the order of **1e** fiber (425 m) > solution (418 nm) > film (401 nm). XRD analysis revealed that **1e** aligns laterally on a glass or silicon surface to form a thin film with a lamella structure; however, it forms a nanofiber with a Lego-like stacking structure without $\pi-\pi$ stacking interaction of the aromatic rings. Reflecting the different nanostructures of the **1e** film and fiber, a spin-coated **1e** film is found to be effective in detecting the vapor of explosives due to the intercalation of nitroaromatics to the cracked surface of the loosely stacked **1e**. In contrast, the **1e** fiber is not effective in detection of nitroaromatics but exhibits fluorescence anisotropy. The maximum fluorescence intensity is obtained in a direction perpendicular to the logitudinal axis of the fiber, indicating the stacking direction to be parallel to the longitudinal axis of the fiber.

Introduction

A variety of photonic materials have been recently reported along with important scientific discoveries of new nanostructures.[1] One of the most important requirements for photonic materials is stability against light and atmospheric oxygen, although many functional π-systems are light- and air-sensitive by nature. Cyclic oligoarylenes have attracted considerable attention among experimental and theoretical chemists,[2] because these molecules exhibit thermal-, light-, and air-stability, unique structures, $\pi-\pi$ interactions, optoelectronic properties, and host ability in host−guest chemistry.[3] In particular, cyclic oligophe-

* Corresponding author. Fax: +81-42-677-2547. Phone: +81-42-677-2525.
† Photonic Research Institute.

10.1021/jo800787u CCC: $40.75
Published on Web 06/21/2008

nylenes bearing medium-size inner cavities are of interest in connection with the unusual properties of open-cage fullerenes.[4] Furthermore, shape- and size-persistent macrocycles with large cavities are attractive targets for synthetic challenges and have potential use in optoelectronics,[5,6] although many difficulties in the synthesis of hardly soluble macrocyclic oligophenylenes prevent detailed studies of their properties.[7] Among them, *o,p,p,o,p,p,o,p,p*-nonaphenylene (**1a**: R = H), a triangular molecule, was first synthesized by Meyer and Staab in 1969 using $CuCl_2$-mediated coupling of the di-Grignard derivative of 4,4″-dibromo-*o*-terphenyl in low yield (0.97%).[2b] In 1984,[2e] Fujioka also obtained **1a** in 5% yield as a byproduct during the intermolecular cross-coupling reaction of di-Grignard reagents of 4,4″-dibromo-*o*-terphenyl and 2,2″-dibromo-*p*-terphenyl with $CuCl_2$ and studied the formation of charge-transfer (CT) complexes of **1a** with either tetracyanoethylene (TCNE) or 2,3-dichloro-5,6-dicyano-*p*-benzoquinone (DDQ).[8] However, further details of properties such as redox behavior, fluorescence quantum yields, incorporation of cationic transition metals, and nanostructure formation have yet to be elucidated for nonaphenylene and its larger counterparts.

For the synthesis of macrocyclic oligoarylenes, transition metal-mediated cross-coupling has been employed in many cases.[9,10] However, aryl−aryl homocoupling forming macrocyclic oligoarylenes has been mainly carried out with use of a combination of aryl Grignard reagent or aryl lithium with $CuCl_2$.[11] In the course of our research on aryl−aryl couplings, we investigated (i) homocoupling of aryl halides with activated nickel complexes,[12] (ii) coupling of arylzinc chloride with $CuCl_2$,[13] and (iii) coupling of arylstannanes with $Cu(NO_3)_2$.[14] Recently, we found a simple and convenient homocoupling of aryl lithium via the electron-transfer oxidation of Lipshutz cuprates with duroquinone that produces biaryls in high yields.[15] Because this new coupling can be expected to have a wide applicability for the synthesis of large-membered oligophenylenes, we employed this procedure for the synthesis of **1a** and its hexaalkyl derivatives **1b**−**d**. We also expected the formation of dodecaphenylenes **2b**−**d**, because the electron-transfer oxidation of Lipshutz cuprates tends to form larger cyclic oligomers than the $CuCl_2$-mediated homocoupling reaction of di-Grignard derivatives.[15,16] This selectivity depends on the structure of the intermediary formed Lipshutz cuprates.[17]

Herein, we report the results of our investigations on the synthesis of nonaphenylenes and dodecaphenylenes using electron-transfer oxidation of Lipshutz cuprates and their unique properties. Although the synthesis of **1a**, **1b**, **1c**, and **2b**, together with the X-ray structure of **1b** has already been reported as a preliminary form,[18] we summarize the results of the oligophenylene synthesis and show further research on the formation of nanostructures from oligophenylenes.

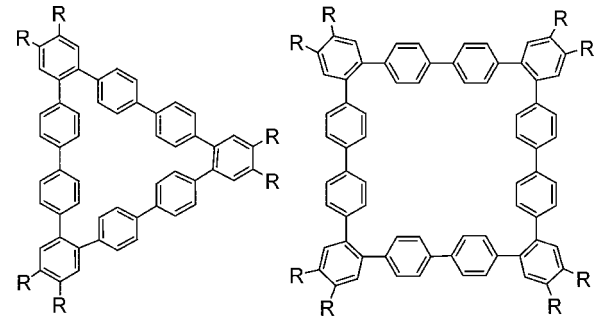

1 **2**

a: R = H **b**: R = Et **c**: R = Bu^n
d: R = $C_8H_{17}{}^n$ **e**: $OC_{12}H_{25}{}^n$

Results and Discussions

Synthesis of Nonaphenylenes 1 and Dodecaphenylenes 2 with Electron-Transfer Oxidation of Lipshutz Cuprates. For the synthesis of hexabutylnonaphenylene **1c**, $CuCl_2$-mediated cyclotrimerization of either the dilithio derivative of **3c** or the bis(chlorozinc) derivative **4c** was first attempted (Scheme 1).[13] Lithiation of **3c** with butyllithium (2 equiv) followed by the reaction with $CuCl_2$ (excess) gave a trace amount of **1c**. In contrast, treatment of **4c** (prepared from dilithio species of **3c** with excess $ZnCl_2$) with $CuCl_2$ (excess) produced hexabutylnonaphenylene **1c** in 20% yield. Although this reaction resulted in the formation of a number of byproducts containing linear oligomers, no formation of octabutyldodecaphenylene **2c** was observed. Unfortunately, however, similar reaction of **3b** with butyllithium, followed by succesive treatment with $ZnCl_2$ and $CuCl_2$ pruduced corresponding **1b** in trace yield.

(1) For recent examples, see: (a) Matsubara, H.; Yoshimoto, S.; Saito, H.; Jianglin, Y.; Tanaka, Y.; Noda, S. *Science* **2008**, *319*, 445–447. (b) Shvets, G. *Nat. Mater.* **2008**, *7*, 7–8. (c) Nesbitt, D. J. *Nature* **2007**, *450*, 1172–1173. (d) Yeom, D.-I.; Eggleton, B. J. *Nature* **2007**, *450*, 953–954. (e) Lu, C.; Dimov, S. S.; Lipson, R. H. *Chem. Mater.* **2007**, *19*, 5018–5022. (f) Busch, K.; von Freymann, G.; Linden, S.; Mingaleev, S. F.; Tkeshelashvili, L.; Wegener, M. *Phys. Rep.* **2007**, *444*, 101–202.

(2) (a) Staab, H. A.; Binnig, F. *Chem. Ber.* **1967**, *100*, 293–305. (b) Meyer, H.; Staab, H. A. *Liebigs Ann.* **1969**, *724*, 30–33. (c) Irngartinger, H.; Leiserowitz, L.; Schmidt, G. M. J. *Chem. Ber.* **1970**, *103*, 1132–1156. (d) Wittig, G.; Rümpler, K.-D. *Liebigs Ann.* **1971**, *751*, 1–16. (e) Fujioka, Y. *Bull. Chem. Soc. Jpn.* **1984**, *57*, 3494–3506. (f) Cram, D. J.; Kaneda, T.; Helgeson, R. C.; Brown, S. B.; Knobler, C. B.; Maverick, E.; Trueblood, K. N. *J. Am. Chem. Soc.* **1985**, *107*, 3645–3657. (g) Chan, C. W.; Wong, H. N. C. *J. Am. Chem. Soc.* **1985**, *107*, 4790–4791. (h) Chan, C. W.; Wong, H. N. C. *J. Am. Chem. Soc.* **1988**, *110*, 462–469. (i) König, B.; Heinze, J.; Meerholz, J. K.; de Meijere, A. *Angew. Chem., Int. Ed.* **1991**, *30*, 1361–1363. (j) Percec, V.; Okita, S. *J. Polym. Sci., Polym. Chem. Ed.* **1993**, *31*, 877–884. (k) Wong, T.; Yuen, M. S. M.; Mak, T. C. W.; Wong, H. N. C. *J. Org. Chem.* **1993**, *58*, 3118–3122. (l) Rajca, A.; Safronov, A.; Rajca, S.; Shoemaker, R. *Angew. Chem., Int. Ed.* **1997**, *36*, 488–491. (m) Hensel, V.; Lützow, K.; Schlüter, A.-D.; Jacob, J.; Gessler, K.; Saenger, W. *Angew. Chem., Int. Ed.* **1997**, *36*, 2654–2656. (n) Kelly, T. R.; Lee, Y.-J.; Mears, R. J. *J. Org. Chem.* **1997**, *62*, 2774–2781. (o) Hensel, V.; Schlüter, A. D. *Chem. Eur. J.* **1999**, *5*, 421–429. (p) Peng, H.-Y.; Lam, C.-K.; Mak, T. C. W.; Cai, Z.; Ma, W.-T.; Li, Y.-X.; Wong, H. N. C. *J. Am. Chem. Soc.* **2005**, *127*, 9603–9611. (q) Stuparu, M.; Gramlich, V.; Stanger, A.; Schlüter, A. D. *J. Org. Chem.* **2007**, *72*, 424–430. (r) Pisula, W.; Kastler, M.; Yang, C.; Enkelmann, V.; Müllen, K. *Chem. Asian J.* **2007**, *2*, 51–56.

(3) (a) Pascal, R. A., Jr. *Chem. Rev.* **2006**, *106*, 4809–4819. (b) Herges, R. *Chem. Rev.* **2006**, *106*, 4820–4842. (c) Wu, Y.-T.; Siegel, J. S. *Chem. Rev.* **2006**, *106*, 4843–4867. (d) Tsefrikas, V. M.; Scott, L. T. *Chem. Rev.* **2006**, *106*, 4868–4884. (e) Kawase, T.; Kurata, H. *Chem. Rev.* **2006**, *106*, 5250–5273. (f) Tahara, K.; Tobe, Y. *Chem. Rev.* **2006**, *106*, 5274–5290. (g) *Carbon-Rich Compounds From Molecules to Materials*; Haley, M. M., Tykwinski, R. R., Eds.; Wiley-VCH: Weinheim, Germany, 2006. (h) *Molecular Devices and Machines*; Balzani, V., Venturi, M., Credi, A., Eds.; Wiley-VCH: Weinheim, Germany, 2003. (i) *Modern Arene Chemistry*; Astruc, D., Ed.; Wiley-VCH: Weinheim, Germany, 2002. (j) *Molecular Switches*; Feringa, B. L., Ed.; Wiley-VCH: Weinheim, Germany, 2001.

(4) (a) Al-Matar, H.; Abdul-Sada, A. K.; Avent, A. G.; Taylor, R. *Org. Lett.* **2001**, *3*, 1669–1671. (b) Murata, Y.; Murata, M.; Komatsu, K. *J. Org. Chem.* **2001**, *66*, 8187–8191. (c) Vougioukalakis, G. C.; Prassides, K.; Orfanopoulos, M. *Org. Lett.* **2004**, *6*, 1245–1247. (d) Stanisky, C. M.; Cross, R. J.; Saunders, M.; Murata, M.; Murata, Y.; Komatsu, K. *J. Am. Chem. Soc.* **2005**, *107*, 299–302. (e) Huang, S.; Wang, F.; Gan, L.; Yuan, G.; Zhou, J.; Zhang, S. *Org. Lett.* **2006**, *8*, 277–247.

(5) (a) Höger, S. *J. Polym. Sci. Part A* **1999**, *37*, 2685–2698. (b) Grave, C.; Schlüter, A. D. *Eur. J. Org. Chem.* **2002**, 807–818. (c) Zhao, D.; Moore, J. S. *Chem. Commun.* **2003**, 807–818. (d) Yamaguchi, Y.; Yoshida, Z. *Chem. Eur. J.* **2003**, *9*, 5430–5440. (e) Höger, S. *Angew. Chem., Int. Ed.* **2005**, *44*, 3806–3808. (f) Schlüter, A. D. *Top. Curr. Chem.* **2005**, *245*, 151–191.

(6) Zhang, W.; Moore, J. S. *Angew. Chem., Int. Ed.* **2006**, *45*, 4416–4439.

(7) (a) Winkler, H. J. S.; Wittig, G. *J. Org. Chem.* **1963**, *28*, 1733–1740. (b) Wittig, G.; Fischer, S.; Günther, R. *Liebigs Ann.* **1973**, 495–498.

(8) Fujioka, Y. *Bull. Chem. Soc. Jpn.* **1985**, *58*, 481–489.

SCHEME 1. Synthesis of Nonaphenylenes 1b,c with $CuCl_2$-Mediated Coupling Reactions

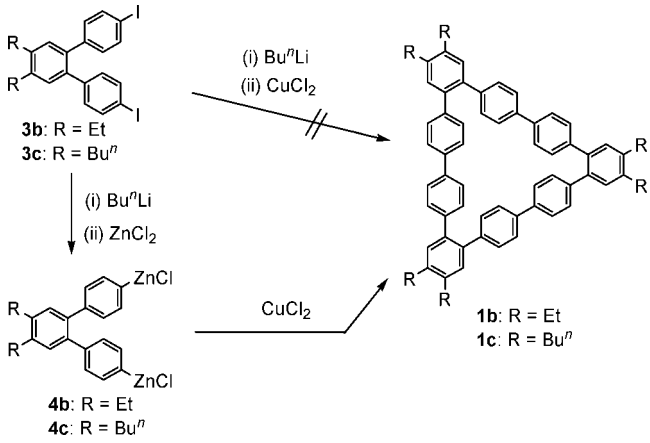

SCHEME 2. Synthesis of Nonaphenylenes 1a,e and Dodecaphenylenes 2b−d

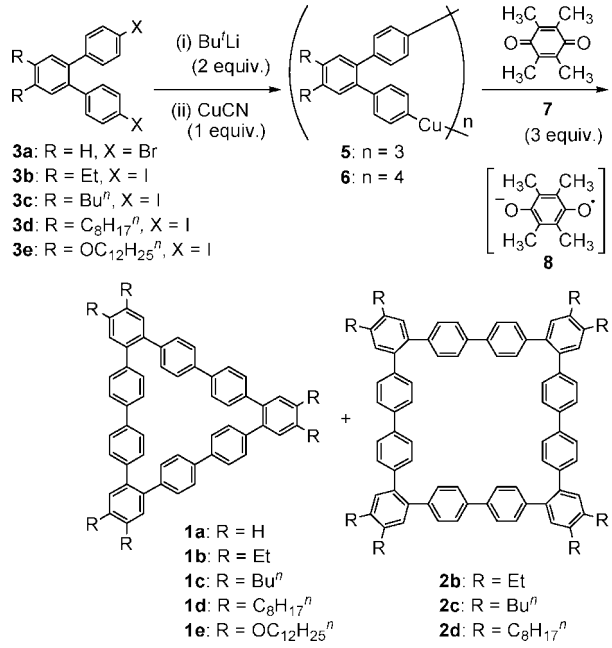

For the synthesis of nonaphenylenes **1** and dodecaphenylenes **2**, we next carried out the electron-transfer oxidation of Lipshutz cuprates, because this reaction is a very effective tool for the formation of aryl−aryl bonds.[15] Thus, the reaction of **3a**−**e** with 2 equiv of *t*-BuLi at −78 °C, followed by treatment with 1 equiv of CuCN in THF (for **3a**) or ether (for **3b**−**e**) at −78 °C to room temperature produced corresponding Lipshutz cuprates **5** and **6**. For the coupling of the cuprate (R = H), electron-transfer oxidation of **5** (R = H) with 3 equiv of duroquinone in THF at room temperature proceeded smoothly to give nonaphenylene **1a** in 46% yield (Scheme 2).

In the case of **3b**−**d** as the starting materials, cyclooligomerization was carried out in ether due to the higher solubility of **3**, **5**, **6**, and related compounds. The electron-transfer oxidation of a mixture of **5b** and **6b** with 3 equiv of duroquinone in ether at −5 °C to room temperature produced **1b** (25%) and **2b** (5%). In a similar manner, the oxidation of Lipshutz cuprates **5** and **6** derived from **3c** and **3d** with duroquinone under similar conditions afforded **1c** (27%) and **1d** (34%), together with **2c** (4%) and **2d** (3%), respectively. However, the oxidation of Lipshutz cuprates derived from **3e** in ether or THF only produced **1e** in 18% and 14% yields, respectively (Scheme 2). Note that the synthesis of oligophenylenes by using the oxidation of Lipshutz cuprates produces rather simple mixtures of cyclic products with small amounts of linear oligomers, although the oligophenylene synthesis with the Ullmann coupling and related reactions sometimes forms complex mixtures of linear oligomers containing small amounts of cyclic products. All nonaphenylenes and dodecaphenylenes synthesized in this work are unreactive to light, atmospheric oxygen, and prolonged heating.[19]

The electron-transfer oxidation of Lipshutz cuprates with excess amounts of duroquinone was examined by ESR measurements. Addition of duroquinone to a yellow solution of Lipshutz cuprates **5** and **6** resulted in a green solution that showed ESR signals due to the durosemiquinone radical **8**.[20] The X-ray structure of **1b** and the calculated structure of **2a** revealed rigid twisting conformations (see the Supporting Information).

Electrochemical Oxidation. Oligophenylenes exhibit π-donor properties.[8] Because nonaphenylenes and dodecaphenylenes form CT-complexes with DDQ to show CT-absorptions at around 750 nm (see Figure S37, Supporting Information), cyclic voltammetric analyses of **1b**−**d** and **2b**−**d** were carried out. Both nonaphenylenes **1b**−**d** and dodecaphenylenes **2b**−**d** showed irreversible oxidations in the range from 1.1 to 1.3 V vs Fc/Fc^+ (Table 1). These moderate oxidation potentials of **1b**−**d** and **2b**−**d** are ascribed to their twisted π-conjugated systems as shown in Figures S23 and S24 in the Supporting Information, although the HOMO orbitals of **1a** and **2a** are spread over all the sp^2-carbons of the molecules (see the Supporting Information). In contrast, hexadodecyloxynonaphenylene **1e** showed quasireversible one-electron oxidation at $E^{ox}_{1/2}$ = 0.70 V due to slightly enhanced stabilization of the cation

(9) Cepanec, I. *Synthesis of Biaryls*; Elsevier: Oxford, UK, 2004.
(10) For recent reviews, see: (a) Negishi, E.-I. *Bull. Chem. Soc. Jpn.* **2007**, *80*, 233–257. (b) de Meijere, A.; Stulgies, B.; Albrecht, K.; Rauch, K.; Wagner, H. A. *Pure Appl. Chem.* **2006**, *78*, 813–830. (c) Zapf, A. *Angew. Chem., Int. Ed.* **2003**, *42*, 5394–5399. (d) Larhed, M.; Moberg, C.; Hallberg, A. *Acc. Chem. Res.* **2002**, *35*, 717–727.
(11) Kauffmann, T. *Angew. Chem.* **1974**, *86*, 321–335.
(12) (a) Iyoda, M.; Otsuka, H.; Sato, K.; Nisato, N.; Oda, M. *Bull. Chem. Soc. Jpn.* **1990**, *63*, 80–87. (b) Iyoda, M.; Sato, K.; Oda, M. *Chem. Commun.* **1985**, 1547–1548. (c) Iyoda, M.; Sato, K.; Oda, M. *Tetrahedron Lett.* **1985**, *26*, 3829–3833.
(13) (a) Iyoda, M.; Kabir, S. M. H.; Vorasingha, A.; Kuwatani, Y.; Yoshida, M. *Tetrahedron Lett.* **1998**, *39*, 5393–5396. (b) Kabir, S. M. H.; Miura, M.; Sasaki, S.; Harada, G.; Kuwatani, Y.; Yoshida, M.; Iyoda, M. *Heterocycles* **2000**, *52*, 761–774. (c) Kabir, S. M. H.; Hasegawa, M.; Kuwatani, Y.; Yoshida, M.; Matsuyama, H.; Iyoda, M. *J. Chem. Soc., Perkin Trans. 1* **2001**, 159–165.
(14) (a) Iyoda, M.; Kondo, T.; Nakao, K.; Hara, K.; Kuwatani, Y.; Yoshida, M.; Matsuyama, H. *Org. Lett.* **2000**, *2*, 2081–2083. (b) Harada, G.; Yoshida, M.; Iyoda, M. *Chem. Lett.* **2000**, 160–161.
(15) (a) Miyake, Y.; Wu, M.; Rahman, M. J.; Iyoda, M. *Chem. Commun.* **2005**, 411–413. (b) Miyake, Y.; Wu, M.; Rahman, M. J.; Kuwatani, Y.; Iyoda, M. *J. Org. Chem.* **2006**, *71*, 6110–6117.
(16) For the electron-transfer oxidation of organometallics, see:(a) Cheng, J.-W.; Luo, F.-T. *Tetrahedron Lett.* **1988**, *29*, 1293–1294. (b) Chen, C.; Xi, C.; Lai, C.; Wang, R.; Hong, X. *Eur. J. Org. Chem.* **2004**, 647–650.
(17) (a) Boche, G.; Bosold, F.; Marsch, M.; Harms, K. *Angew. Chem., Int. Ed.* **1998**, *37*, 1684–1686. (b) Kronenburg, C. M. P.; Jastrzebski, J. T. B. H.; Spek, A. L.; van Koten, G. *J. Am. Chem. Soc.* **1998**, *120*, 9688–9689. (c) Krause, N. *Angew. Chem., Int. Ed.* **1999**, *38*, 79–81. (d) Hwang, C.-S.; Power, P. P. *J. Am. Chem. Soc.* **1998**, *120*, 6409–6410.
(18) Iyoda, M.; Rahman, M. J.; Matsumoto, A.; Wu, M.; Kuwatani, Y.; Nakao, K.; Miyake, Y. *Chem. Lett.* **2005**, *34*, 1474–1475.
(19) Nonaphenylenes **1a**−**e** and dodecaphenylenes **2b**−**d** were recovered unchanged after either exposure of the $CDCl_3$ solutions to sunlight for several hours or prolonged heating at 160 °C under air. The thermal gravity (TG) analysis of **1e** showed the decomposition at 350 °C.
(20) (a) Giordani, R.; Buc, J. *Eur. J. Biochem.* **2004**, *271*, 2400–2407. (b) Pasimeni, L.; Brustolon, M.; Corvaja, C. *J. Chem. Soc., Faraday Trans. 2* **1972**, *68*, 223–233. (c) Gough, T. E.; Hindle, P. R. *Can. J. Chem.* **1969**, *47*, 1698–1700.

TABLE 1. Oxidation Potentials of 1b−d and 2b−d[a]

compd	E^{ox} (V)	compd	E^{ox} (V)
1b	1.30	**2b**	1.12
1c	1.19	**2c**	1.14
1d	1.17	**2d**	1.15

[a] Conditions: 0.1 M *n*-BuN_4ClO_4, glassy carbon working electrode, and Pt counter electrode in 1,2-dichlorobenzene at 23 °C. Potentials were measured against Ag/Ag^+ electrode and converted to the value vs Fc/Fc^+.

TABLE 2. UV−Vis and Fluorescence Spectral Data of 1a−e and 2b−d in THF

compd	λ_{abs} [nm] (log ϵ)	λ_{em} [nm]	Φ_F[a]
1a[b]	283 (4.97), 322 sh (4.39)	392	0.60
1b[b]	288 (5.01), 325 sh (4.48)	400	0.92
1c[b]	288 (4.89), 323 sh (4.41)	400	0.98
1d[b]	289 (5.04), 326 sh (4.53)	393	0.93
1e[b]	295 (5.09)	418	0.95
2b	297 (5.09)	393	0.91
2c	298 (4.92)	391	0.99
2d	298 (5.15)	393	0.95

[a] Fluorescence quantum yield (Φ_F) was determined by comparison with quinine sulfate in 0.5 M H_2SO_4 ($\Phi_F = 0.546$). [b] Analytically pure sample was used.

radical species with hexadodecyloxy units. Note that dodecaphenylenes **2b−d** show slightly lower oxidation potentials than nonaphenylenes **1b−d**. These differences in oxidation potential are consistent with the calculated HOMO levels (B3LYP/6-31G(d)) of **1a** (−5.577 eV) and **2a** (−5.474 eV).

Electronic Absorption and Emission Spectra. As expected for the phenylene system,[21] the cyclic oligophenylenes **1b−d** and **2b−d** show strong UV−vis absorption at around 300 nm and strong fluorescent emission at around 400 nm with high quantum yields (see the Supporting Information). As shown in Table 2, the electronic spectra of **1b−d** and **2b−d** show strong absorption maxima at 288−289 (log ϵ = 4.89−5.04) and 297−298 (log ϵ = 4.92−5.15) nm, respectively. The fluorescence spectra of **1b** and **2b** exhibit emissions at 393−400 (Φ_F = 0.92−0.98) and 391−393 (Φ_F = 0.91−0.99) nm, respectively. As **2b−d** have a larger π system than **1b−d**, the absorption maxima of **2b−d** shift to longer wavelengths than those of **1b−d**. In contrast, the emissions of **1b−d** shift to longer wavelengths than those of **2b−d**. In the case of **1e**, the absorption and emission maxima exhibit a red shift due to the electron-donating properties of dodecyloxy groups (see the Supporting Information). Interestingly, the emissions of **1** and **2** show a solvent effect (quenching of emission). Thus, the quantum yields (Φ_F) of **1b** in $CHCl_3$ and CCl_4 were reduced to 0.88 and 0.013, respectively, probably due to electron transfer from the excited **1b** to $CHCl_3$ and CCl_4 (see the Supporting Information).[22] Since nonaphenylenes **1b−d** and dodecaphenylenes **2b−d** are π-donor systems with inner cavities, they shows inclusion behavior with silver salts[23] and dynamic complexation[24] (see the Supporting Information).

Nanostructures Based on Self-Assembled 1e. Nanostructured, one-dimensional (1D) and two-dimensional (2D) morphologies composed of amphiphilic molecules have received increasing attention,[25] and electrically active π-conjugated molecules have been employed for the formation of nanowires and nanotubes.[26,27] In contrast with nanostructures from amphiphilic molecules without a hydrogen bonding site, large planar molecular surfaces are believed to be essential for promoting $\pi-\pi$ stacking interaction, together with long alkyl chains and polarized aromatic groups.[28] Interestingly, however, nonaphenylene **1e** having neither a planar frame nor strong polar groups forms nanostructures on the surface and in solution.[29]

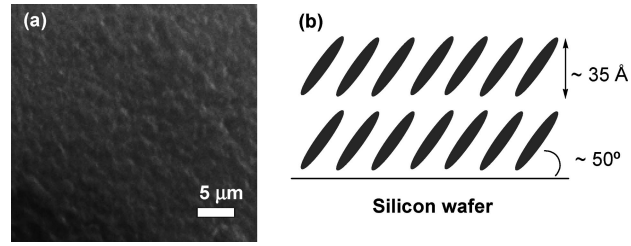

FIGURE 1. (a) SEM image of **1e** film. (b) Schematic representation of the film structure of **1e**.

Uniform spin-coated **1e** films were prepared on glass or silicon wafer by casting a 1.0 mM solution of **1e** in cyclohexane, benzene, chloroform, THF, or diidopropyl ether (IPE). The SEM and X-ray diffraction (XRD) measurements of the film revealed a laterally ordered lamellar structure (d = 34.5 Å) that rises 50° diagonally from the surface of silicon wafer (Figures 1 and 2). Diffractograms of grazing incidence X-ray reflectivity (GIXR) and in-plane XRD of a film prepared from a THF solution of **1e** showed the thickness of the film to be ∼22 nm and the presence of loose $\pi-\pi$ stacking (4.4 Å), respectively (see the Supporting Information).

In contrast to the film, **1e** forms a fibrous material from IPE−methanol (1:1), although **1e** shows no self-aggregation in

(21) (a) Cao, X.-Y.; Zi, H. Y.; Zhang, W.; Lu, H.; Pei, J. *J. Org. Chem.* **2005**, *70*, 3645–3653. (b) Holman, M. W.; Liu, R.; Zang, L.; Yan, P. *J. Am. Chem. Soc.* **2004**, *126*, 16126–16133. (c) Li, Z. H.; Wong, M. S.; Tao, Y.; D'Iorio, M. *J. Org. Chem.* **2004**, *69*, 921–927.

(22) Bonesi, S. M.; Erra-Balsells, R. *J. Chem. Soc., Perkin Trans. 2* **2000**, 1583–1595.

(23) (a) Munakata, M.; Wu, L. P.; Ning, G. L.; Kuroda-Sowa, T.; Maekawa, M.; Suenaga, Y.; Maeno, N. *J. Am. Chem. Soc.* **1999**, *121*, 4968–4976. (b) Iyoda, M.; Kuwatani, Y.; Yamauchi, T.; Oda, M. *Chem. Commun.* **1988**, 65–66. (c) Iyoda, M.; Horino, T.; Takahashi, F.; Hasegawa, M.; Yoshida, M.; Kuwatani, Y. *Tetrahedron Lett.* **2001**, *42*, 6883–6886.

(24) (a) Pierre, J.-L.; Baret, P.; Chautemps, P.; Armand, M. *J. Am. Chem. Soc.* **1981**, *103*, 2986–2988. (b) Kang, H. C.; Hanson, A. W.; Eaton, B.; Boekelheide, V. *J. Am. Chem. Soc.* **1985**, *107*, 1979–1985. (c) Sirinintasak, S.; Kuwatani, Y.; Hoshi, S.; Isomura, E.; Nishinaga, T.; Iyoda, M. *Tetrahedron Lett.* **2007**, *48*, 3433–3436.

(25) (a) Ajyayaghosh, A.; Praveen, V. K. *Acc. Chem. Res.* **2007**, *40*, 644–656. (b) Shimizu, T.; Masuda, M.; Minamikawa, H. *Chem. Rev.* **2005**, *105*, 1401–1443. (c) Hoeben, F. M. J.; Jonkheijm, P.; Meijer, E. W.; Schenning, A. P. H. J. *Chem. Rev.* **2005**, *105*, 1491–1546. (d) Grimsdale, A. C.; Müllen, K. *Angew. Chem., Int. Ed.* **2005**, *44*, 5592–5629. (e) Ishi-i, T.; Shinkai, S. *Top. Curr. Chem.* **2005**, *258*, 119–160. (f) Sangeetha, N. M.; Maitra, U. *Chem. Soc. Rev.* **2005**, *34*, 821–836.

(26) (a) Yamamoto, Y.; Fukushima, T.; Suna, Y.; Ishii, N.; Saeki, A.; Seki, S.; Tagawa, S.; Taniguchi, M.; Kawai, T.; Aida, T. *Science* **2006**, *314*, 1761–1764. (b) Sly, J.; Kasák, P.; Gomar-Nadal, E.; Rovira, C.; Górriz, L.; Thorarson, P.; Amabilino, D. B.; Rowan, A. E.; Nolte, R. J. M. *Chem. Commun.* **2005**, 1255–1257. (c) Akutagawa, T.; Kakiuchi, K.; Hasegawa, T.; Noro, S.; Nakamura, T.; Hasegawa, H.; Mashiko, S.; Becher, J. *Angew. Chem., Int. Ed.* **2005**, *44*, 7283–7287. (d) Kitamura, T.; Nakaso, S.; Mizoshita, N.; Tochigi, Y.; Shimomura, T.; Moriyama, M.; Ito, K.; Kato, T. *J. Am. Chem. Soc.* **2005**, *127*, 14769–14775. (e) Puigmarti-Luis, J.; Laukhin, V.; Del Pino, A. P.; Vidal-Gancedo, J.; Rovira, C.; Laukhina, E.; Amabilino, D. B. *Angew. Chem., Int. Ed.* **2007**, *46*, 238–241.

(27) (a) Hasegawa, M.; Enozawa, H.; Kawabata, Y.; Iyoda, M. *J. Am. Chem. Soc.* **2007**, *129*, 3072–3073. (b) Kobayashi, Y.; Hasegawa, M.; Enozawa, H.; Iyoda, M. *Chem. Lett.* **2007**, *36*, 720–721. (c) Nakao, K.; Nishimura, M.; Tamachi, T.; Kuwatani, Y.; Miyasaka, H.; Nishinaga, T.; Iyoda, M. *J. Am. Chem. Soc.* **2006**, *128*, 16740–16747.

(28) (a) Kastler, M.; Pisula, W.; Wasserfallen, D.; Pakula, T.; Müllen, K. *J. Am. Chem. Soc.* **2005**, *127*, 4286–4296. (b) Balakrishnan, K.; Datar, A.; Zhang, W.; Yang, X.; Naddo, T.; Huang, J.; Zuo, J.; Yen, M.; Moore, J. S.; Zang, L. *J. Am. Chem. Soc.* **2006**, *128*, 6576–6577. (c) Enozawa, H.; Hasegawa, M.; Takamatsu, D.; Fukui, K.; Iyoda, M. *Org. Lett.* **2006**, *8*, 1917–1920.

(29) Although **1e** forms nanostructures, **1a**, **1b**, and **2b** precipitate as crystals and **1c**, **1d**, **2c**, and **2d** form microcrystals from solution.

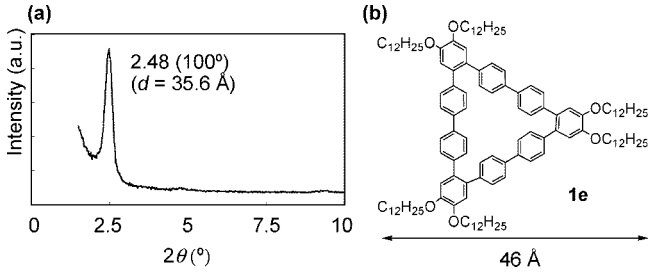

FIGURE 2. (a) XRD pattern of **1e** film on an aluminum plate. (b) Molecular size of **1e**.

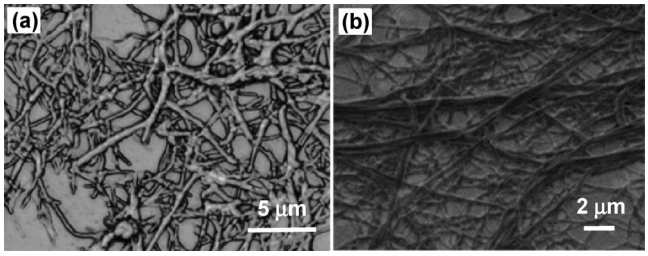

FIGURE 3. Microscopy images of **1e**. (a) Optical micrograph on a glass plate using a confocal laser scanning microscope. (b) SEM image of **1e** threads on a silicon wafer.

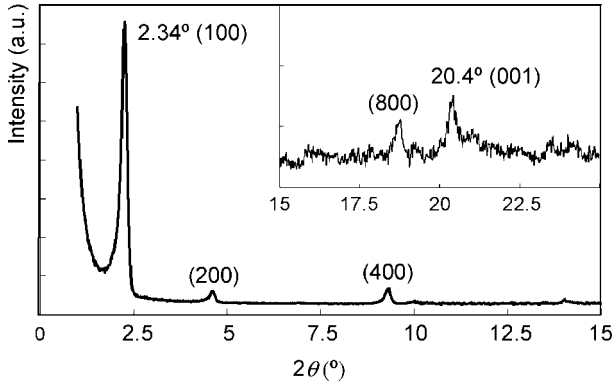

FIGURE 4. XRD pattern of **1e** fiber; the inset shows the region $15° < 2\theta < 25°$.

common organic solvents. Thus, **1e** (10 mg) was dissolved in 1 mL of diisopropyl ether−methanol (1:1) and allowed to stand for several hours at room temperature to form a stringy material that was cast on a glass plate. Microscopy images clearly show a fibrous structure of this material (Figure 3), and an SEM image of the **1e** fiber shows a structure of entangled molecular wires of 100−500 μm width and 100−160 nm thickness (Figure 3b).

The result of the XRD analysis of the **1e** fiber showed a regular reflection pattern, and a distinct (100) peak at $2\theta = 2.34°$ (d = 37.8 Å) together with three higher order reflections observed in a small-angle region, indicating considerably high crystallinity and the existence of a lamellar structure of 3.78 nm (37.8 Å) pitch (Figure 4). Moreover, a weak (001) peak at $2\theta = 20.4°$ (4.3 Å) revealed a stacking structure without $\pi-\pi$ interaction probably similar to the packing structure of **1b** (Supporting Information). Since the molecular size of **1e** was estimated to be ca. 46 Å, the molecules are arranged with lateral alkoxy−alkoxy interaction to form a sheet structure together with stacking of the nonaphenylene core.

On the base of the strong emission of **1e** in solution and the packing mode of the fibrous material, the **1e** fiber is determined to have a fluorescence anisotropy. As shown in panels b and c

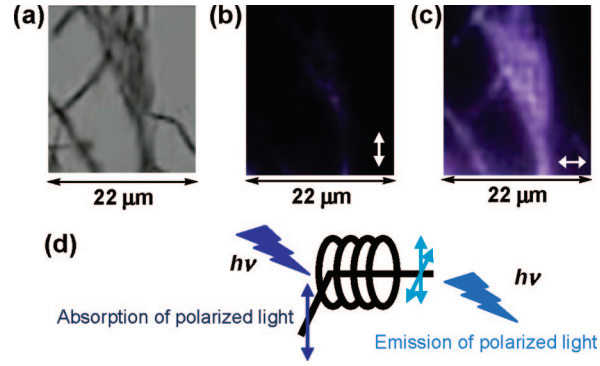

FIGURE 5. (a) Microscopic transmission image of the fibers of **1e** on glass plate. (b and c) Fluorescence images of the same part of sample excited by UV light (355 nm) with different directions of linear polarization (indicated by a double headed arrow). (d) Excitation with polarized light (deep blue arrow) and corresponding spontaneous emission (light blue arrow).

of Figure 5, maximum fluorescence intensity is obtained when the polarization direction is perpendicular to the direction of the fiber. This result suggests that the transition dipole moments of **1e** are aligned perpendicular to the direction of the fiber. As the transition dipole moment of **1e** is parallel to the molecular plane, the stacking direction is considered to be parallel to the direction of the fiber (Figure 5d). Since the crystal structure of **1b** shows a stacking structure without strong $\pi-\pi$ interaction (Figure S23, Supporting Information), **1e** forms a nanofiber with a Lego-like stacking structure of the aromatic rings. The high fluorescence quantum yield ($\Phi_F = 0.53$) of the **1e** fiber also supports small $\pi-\pi$ interaction in the nanostructure.

Among a variety of methods of explosive detection,[30] fluorescence quenching is one of the most sensitive and convenient methods, and porous films prepared from aromatic compounds and conjugated polymers have been reported as an effective sensor.[31] Although the fluorescence of **1e** in solution is effectively quenched with nitroaromatics such as 1,3-dinitrobenzene (DNB), 2,4-dinitrotoluene (DNT), and 1,3,5-trinitrobenzene (TNB), the **1e** fiber and film show a different behavior toward vaporized nitroaromatics. Thus, the **1e** fiber is proven to be ineffective in sensing nitroaromatic vapor in contrast to the result obtained for arylene−ethynylene tetracycle.[31f] Interestingly, the **1e** film, however, is found to be effective in sensing DNB and DNT because of the different stacking modes of the **1e** fiber and film. Thus, a film prepared on a quartz plate is fluorescent (quantum yield: $\Phi_F = 0.12$). As shown in Figure 6, the fluorescence of the **1e** film was rapidly quenched by exposing it to saturated DNT vapor. To examine the structure of DNT-doped **1e** film, XRD and in-plane XRD analyses were carried out. However, no change in XRD and in-plane XRD patterns were observed, indicating no structural change of the **1e** film. Due to lose intercalation of DNT in the

(30) (a) Fainberg, A. *Science* **1992**, *255*, 1531–1537. (b) Swager, T. M. *Acc. Chem. Res.* **1998**, *31*, 201–207. (c) Steinfeld, J. I.; Wormhoudt, J. *Annu. Rev. Phys. Chem.* **1998**, *49*, 203–232.

(31) (a) Yang, J.-S.; Swager, T. M. *J. Am. Chem. Soc.* **1998**, *120*, 11864–11873. (b) Chen, L.; McBranch, D.; Wang, R.; Whitten, D. *Chem. Phys. Lett.* **2000**, *330*, 27–33. (c) Sohn, H.; Sailor, M. J.; Magde, D.; Trogler, W. C. *J. Am. Chem. Soc.* **2003**, *125*, 3821–3830. (d) Liu, Y.; Mills, R. C.; Boncella, J. M.; Schanze, K. S. *Langmuir* **2001**, *17*, 7452–7455. (e) Goldman, E. R.; Medintz, I. L.; Whitley, J. L.; Hayhurst, A.; Clapp, A. R.; Uyeda, H. T.; Deschamps, J. R.; Lassman, M. E.; Mattoussi, H. *J. Am. Chem. Soc.* **2005**, *127*, 6744–6781. (f) Naddo, T.; Che, Y.; Zhang, W.; Balakrishnan, K.; Yang, X.; Yen, M.; Zhao, J.; Moore, J. S.; Zang, L. *J. Am. Chem. Soc.* **2007**, *129*, 6978–6979. (g) Narayanan, A.; Varnavski, O. P.; Swager, T. M.; Goodson, T., III *J. Phys. Chem. C* **2008**, *112*, 881–884.

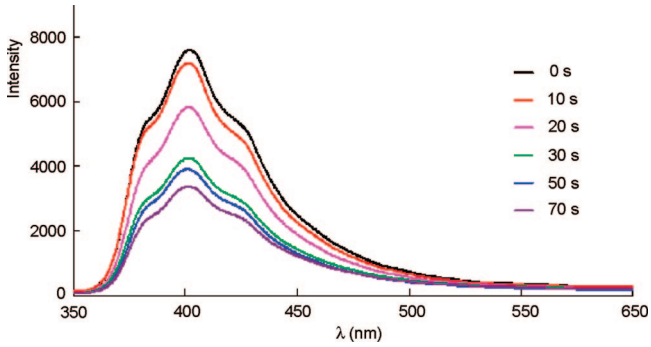

FIGURE 6. Time-dependent fluorescence spectra of spin-coated film (24 nm thick) of **1e** after exposure to saturated vapor of 2,4-dinitrotoluene (λ_{ex} = 316 nm) at 25 °C.

1e film, DNT can be removed under reduced pressure for 1 h to achieve regeneration of 98% emission.[32] Similarly, the **1e** film can be employed for detecting a vaporized DNB (see the Supporting Information).

Conclusion

The synthesis of nonaphenylenes **1a**−**e** and dodecaphenylenes **2b**−**d** highly unreactive to heat, light, and air oxidation with use of electron-transfer oxidation of the corresponding Lipshutz cuprates was carried out. One-pot reaction starting from 4,4″-dihalo-*o*-terphenyls via the formation of macrocyclic cuprate intermediates in ether or THF produced nonaphenylenes and dodecaphenylenes in moderate total yields. Synthesized oligophenylenes **1b**−**e** and **2b**−**d** exhibited UV−vis absorption at around 300 nm and strong blue emission at around 400 nm with high quantum yields (Φ_F > 90%) except for **1a** (Φ_F = 60%); **2b**−**d** with a larger π-system showed a longer absorption maxima than **1b**−**d**, whereas the fluorescent emissions of **1b**−**d** shifted to a longer wavelength than those of **2b**−**d**. Smaller Stokes-shifts in **2b**−**d** (93−96 nm) than those in **1b**−**d** (104−112 nm) reflect a slightly smaller HOMO−LUMO gap of **2b**−**d**. Oligophenylenes with alkyl substituents reveal irreversible oxidation (E^{ox} = 1.1−1.3 V) under CV analysis, while hexadodecyloxynonaphenylene **1e** shows quasireversible oxidation ($E^{ox}_{1/2}$ = 0.70 V) under similar conditions. The most interesting property of oligophenylenes is the different nanostructures of **1e** on the surface and in solution. The XRD analyses on the **1e** film revealed a loosely aligned lamellar structure rising 50° diagonally from the surface, whereas the fibrous material of **1e** indicates a fairly high crystallinity probably due to lateral alkoxy−alkoxy interaction. The **1e** fiber consists of a sheet structure of 3.78 nm (37.8 Å) pitch perpendicular to the fiber direction and the intermolecular perpendicular distance between the phenyl rings at the apex position is 4.3 Å, indicating no π−π stacking interaction and a Lego-like interlocking structure. Consistent with these structural assumptions, the **1e** fiber shows an anisotropic fluorescence in polarized light with fairly high fluorescence quantum yield (Φ_F = 53%). The most remarkable property of the **1e** film is detection of vaporized nitroaromatics such as DNB and DNT. The fluorescence of the **1e** film decreases very quickly under exposure to nitroaromatic vapor but reverts under reduced pressure for 1 h. Since oligophenylenes are extremely stable functional materials, our new approach to the synthesis and nanostructures of oligophenylenes could be extended to interesting multifunctional materials through control of the structural, optoelectronic, and device properties.

(32) Under reduced pressure (~2 mmHg) for 1 h, over 98% of emission of the **1e** film was regenerated (see the Supporting Information).

Experimental Section

Synthesis of *o*,*p*,*p*,*o*,*p*,*p*,*o*,*p*,*p*-Nonaphenylene 1a with Electron-Transfer Oxidation of 5a. To a solution of **3a** (194 mg, 0.5 mmol) in dry THF (60 mL) was added *t*-BuLi (0.76 mL, 1.1 mmol, 1.44 M in *n*-pentane) at −78 °C under nitrogen atmosphere. The mixture was stirred at the same temperature for 1.5 h, and CuCN (45 mg, 0.5 mmol) was added. The reaction mixture was then allowed to stand at room temperature with vigorous stirring until all the CuCN was completely dissolved. Then, 2,3,5,6-tetramethyl-1,4-benzoquinone (246 mg, 1.5 mmol) was added and the mixture was stirred for 3 h at room temperature. After the completion of the reaction, water was added followed by the addition of benzene. The organic layer was separated and the aqueous layer was extracted with benzene. The combined organic layer was dried over anhydrous $MgSO_4$, and the solvent was evaporated in vacuo to give a crude product. The product was chromatographed by silica gel with cyclohexane/benzene (3/1) as eluent to afford **1a** (53 mg, 46% yield) as colorless crystals, mp 490 °C (lit.[1e] mp 488 °C); ^{1}H NMR (500 MHz, $CDCl_3$) δ 7.50 (12H, d, J = 8.3 Hz), 7.48 (6H, dd, J = 5.8, 3.4 Hz), 7.44 (6H, dd, J = 5.8, 3.4 Hz), 7.16 (12H, d, J = 8.3 Hz); ^{13}C NMR (125 MHz, $CDCl_3$) δ 140.7, 140.6, 137.6, 130.1, 129.9, 127.4, 125.7; UV (THF) λ_{max} (log ε) 283 (4.97), 322 sh (4.39) nm; MS (LDI-TOF) *m*/*z* 684 (M^+).

General Procedure for the Synthesis of Alkyl-Substituted Nonaphenylenes 1b−d and Codecaphenylenes 2b−d. To a solution of **3a**−**e** (0.5 mmol) in dry ether (60 mL) was added *t*-BuLi (1.1 mmol) at −78 °C under nitrogen atmosphere. The mixture was stirred at the same temperature for 1.5 h, and CuCN (45 mg, 0.5 mmol) was added. The reaction mixture was then allowed to stand at room temperature with vigorous stirring until all the CuCN was completely dissolved. 2,3,5,6-Tetramethyl-1,4-benzoquinone (246 mg, 1.5 mmol) was added, and the mixture was stirred for 3 h at room temperature. After the completion of the reaction, water was added, followed by the addition of benzene. The organic layer was separated and the aqueous layer was extracted with benzene. The combined organic layer was dried over $MgSO_4$, and the solvent was evaporated to give a crude product. Nonaphenylenes and dodecaphenylenes were separated by column chromatography on silica gel with cyclohexane/benzene (3:1) as eluent.

Hexaoctylnonaphenylene (1d) and Octaoctyldodecaphenylene (2d). Yield of **1d** 179 mg (34%), colorless fine crystals, mp 60−62 °C; ^{1}H NMR (500 MHz, $CDCl_3$) δ 7.49 (12H, d, J = 8.3 Hz), 7.27 (6H, s), 7.15 (12H, d, J = 8.3 Hz), 2.77 (12H, t, J = 7.9 Hz), 1.69−1.63 (12H, m), 1.46−1.41 (12H, m), 1.38−1.24 (48H, m), 0.89 (18H, t, J = 7.3 Hz); ^{13}C NMR (125 MHz, $CDCl_3$) δ 140.7, 139.9, 138.0, 137.4, 130.6, 130.2, 125.6, 32.5, 31.9, 31.3, 29.9, 29.5, 29.3, 22.7, 14.1; UV (THF) λ_{max} (log ε) 289 (5.04), 326 sh (4.53) nm; MS (LDI-TOF) *m*/*z* 1358 (M^+). Anal. Calcd for $C_{102}H_{132}$: C, 90.20; H, 9.80. Found: C, 90.36; H, 9.64. Yield of **2d** 16 mg (3%), colorless fine crystals, mp 72−74 °C; ^{1}H NMR (500 MHz, CD_2Cl_2) δ 7.45 (16H, d, J = 8.2 Hz), 7.27 (8H, s), 7.24 (16H, d, J = 8.2 Hz), 2.70 (16H, t, J = 8.2 Hz), 1.69−1.62 (16H, m), 1.49−1.26 (80H, m), 0.90 (24H, t, J = 7.3 Hz); ^{13}C NMR (125 MHz, CD_2Cl_2) δ 140.9, 140.7, 139.2, 137.4, 132.0, 130.6, 126.8, 32.8, 32.3, 31.9, 30.2, 29.9, 29.7, 23.1, 14.1; UV (THF) λ_{max} (log ε) 298 (5.15) nm; MS (LDI-TOF) *m*/*z* 1810 (M^+ + 1); HRMS (*m*/*z*) calcd for $^{12}C_{135}{}^{13}CH_{176}$ 1810.3805, found 1810.3873 (M^+ + 1).

Synthesis of Hexadodecyloxynonaphenylene (1e). Synthesis of **1e** in ether or THF was carried out by using a similar procedure to the synthesis of **1b**−**d**: **3e** (197 mg, 0.23 mmol) with *t*-BuLi (0.74 mL of 1.49 M pentane solution, 1.1 mmol), CuCN (23 mg, 0.25 mmol), and 2,3,5,6-tetramethyl-1,4-benzoquinone (114 mg, 0.70 mmol). Yield 25 mg (18%), colorless powder, mp 80−88 °C;

^{1}H NMR (500 MHz, $CDCl_3$) δ 7.47 (12H, d, J = 8.5 Hz), 7.13 (12H, d, J = 8.5 Hz), 7.00 (6H, s), 4.07 (12H, t, J = 6.5 Hz), 1.89−1.82 (12H, m), 1.51−1.45 (12H, m), 1.40−1.22 (96H, m), 0.88 (18H, t, J = 7.0 Hz); ^{13}C NMR (125 MHz, $CDCl_3$) δ 148.1, 140.5, 137.3, 133.1, 130.1, 125.5, 115.4, 69.5, 32.0, 29.80, 29.75, 29.74, 29.51, 29.46, 29.42, 26.15, 22.79, 14.24; UV (THF) λ_{max} (log ε) 302 (5.09) nm; MS (LDI-TOF) m/z 1790.5 (M^+). Anal. Calcd for $C_{126}H_{180}O_6$: C, 84.51; H, 10.13. Found: C, 84.39; H, 10.32.

Fluorescence Anisotropy Studies. Transmission/fluorescence microscopy images were obtained with an OLYMPUS BX50 microscope with a 40× objective lens (N.A. 0.75). As the excitation source, a COHERENT AVIA355 laser was used. The excitation beam from the laser (λ = 355 nm, pulse width ∼30 ns, repetition rate 60 kHz) was led to the microscope with a chromic half-mirror, and then made to irradiate the sample. The excitation power was adjusted by a variable neutral density (rND) filter placed in the optical path between the laser and the microscope. The pulse energy used for the imaging was less than 3 μJ. The polarization direction was controlled by rotating a Fresnel-Rhombs half-wave retarder placed after the rND filter. The emission from the sample was collected by the same objective lens and the images were recorded by a CCD attached to the microscope.

Acknowledgement. This work was supported in part by CREST of JST (Japan Science and Technology Corporation) and by a Grant-in-Aid for Scientific Research from the Ministry of Education, Culture, Sports, Science and Technology, Japan. We would like to thank Prof. Takayuki Kawashima and Prof. Naokazu Kano (University of Tokyo) for the measurements of high resolution mass spectra, Mr. Satoshi Yoshimi and Mr. Takenao Fujii (SHIMADZU Corporation) for the measurements of confocal laser scanning microscopy and SEM images, and Ms. Ayako Morishima and Mr. Takashi Yamaguchi (JASCO Corporation) for the measurements of fluorescence quantum yields of the fiber and film of **1e**. We are grateful to Dr. Yoshihiro Miyake (University of Tokyo), Dr. Yoshiyuki Kuwatani (VSN Inc.), Dr. Kazumi Nakao (Mitsubishi Chemical Co.), and Dr. Mo Wu (Wako Pure Chemical Industries, Ltd.) for their helpful discussions.

Supporting Information Available: Experimental details for all new compounds; copies of ^{1}H and ^{13}C NMR spectra; X-ray data of **1b**; cyclic voltammograms, absorption and emission data, and silver complex formation; microscopy images of fibers; and computational details. This material is available free of charge via the Internet at http://pubs.acs.org.

JO800787U